INFORMATION TECHNOLOGY, COMPUTER SCIENCE AND MANAGEMENT
ИНФОРМАТИКА, ВЫЧИСЛИТЕЛЬНАЯ ТЕХНИКА И УПРАВЛЕНИЕ

UDC 538.915;538.958
https://doi.org/10.23947/2687-1653-2025-25-2-129-141

Original Theoretical Research

Ab initio Calculations of the Electronic-Energy Structure and Optical Properties of Lanthanum and Neodymium Pyrozirconates

EDN: MJOLRM

Anatoliy A. Lavrentyev[1] ✉, **Boris V. Gabrelian**[1], **Vu Van Tuan**[2], **Ksenia F. Kalmykova**[1]

[1] Don State Technical University, Rostov-on-Don, Russian Federation
[2] Institute for Computational Science and Artificial Intelligence, Van Lang University, Ho Chi Minh City, Vietnam
✉ alavrentyev@donstu.ru

Abstract

Introduction. Compounds with lanthanum and neodymium ($La_2Zr_2O_7$ and $Nd_2Zr_2O_7$) have low thermal conductivity, high permittivity and melting point, stability and resistance to defects. They can be used for thermal insulation of metal components in turbines and air engines. Also, these compounds are widely studied from the point of view of the development of materials science, particularly, for the improvement of laser technology and optics. However, the physical properties of $La_2Zr_2O_7$ and $Nd_2Zr_2O_7$ have not been sufficiently studied experimentally. This gap is intended to be filled by the presented study. The research objective includes model calculations of the electronic structure and optical properties of $La_2Zr_2O_7$ and $Nd_2Zr_2O_7$.

Materials and Methods. Based on model calculations within the framework of the density functional theory, the electron-energy structure of pyrozirconates $La_2Zr_2O_7$ and $Nd_2Zr_2O_7$, containing Zr and having the crystal structure of pyrochlore was investigated. The parameters of the crystal lattice of $La_2Zr_2O_7$ taken from the literature were used in the calculations. Due to the lack of experimental data, the parameters for $Nd_2Zr_2O_7$ were calculated by minimizing the forces acting on the atoms of the compound. A combined exchange-correlation potential was used, taking into account the strong interactions of *d*- and *f*-electrons of La and Nd atoms with a correction in the form of a modified Becke-Johnson meta-potential. *Wien2K* software package was used for the calculations.

Results. The densities of electron states of all atoms of the studied compounds were obtained. The calculated densities of valence electron states of the compounds were compared to the experimental X-ray photoelectron spectra. At zero energy, the optical characteristics of $La_2Zr_2O_7$ and $Nd_2Zr_2O_7$ were calculated. Firstly, it was the permittivity: for $La_2Zr_2O_7$ — 8.4334, for $Nd_2Zr_2O_7$ — 8.501; secondly, refraction: for $La_2Zr_2O_7$ — 2.904, for $Nd_2Zr_2O_7$ — 2.916; thirdly, reflection: for $La_2Zr_2O_7$ — 23.786%, for $Nd_2Zr_2O_7$ — 23.935%. High optical absorption coefficient (>10^5 cm^{-1}) was recorded in the ranges: from 5 to 14 eV, from 14 to 28 eV, and from 28 to 40 eV. Peak extinction values were in the ranges from 5 to 13 eV, from 14 to 28 eV, and from 28 to 40 eV. $La_2Zr_2O_7$ and $Nd_2Zr_2O_7$ crystals could absorb photons in a wide energy range (4–10 eV).

Discussion and Conclusion. The study supplemented the concept of the properties of $La_2Zr_2O_7$ and $Nd_2Zr_2O_7$ with new experimental data. The densities of electron states and optical spectra of $La_2Zr_2O_7$ and $Nd_2Zr_2O_7$ compounds were calculated. This made it possible to explain features of the experimental X-ray photoelectron spectra of the compounds. In the approximation of the modified Becke-Johnson potential, the values of the widths of the forbidden bands of the compounds corresponding to the experimental ones were obtained. The research is fundamental and can open up prospects for creating more efficient, reliable and functional materials, laser and optical devices.

Keywords: electron energy structure, properties of the pyrochlore group, modified Becke-Johnson meta-potential, lanthanum and neodymium pyrozirconates, optical properties of $La_2Zr_2O_7$ and $Nd_2Zr_2O_7$, X-ray photoelectron spectra

Acknowledgments. The authors would like to thank the reviewers, whose critical evaluation of the submitted materials and suggestions for improvement contributed significantly to the quality of this article.

For Citation. Lavrentyev AA, Gabrelian BV, Vu Van Tuan, Kalmykova KF. *Ab initio* Calculations of the Electronic-Energy Structure and Optical Properties of Lanthanum and Neodymium Pyrozirconates. *Advanced Engineering Research (Rostov-on-Don).* 2025;25(2):129–141. https://doi.org/10.23947/2687-1653-2025-25-2-129-141

Оригинальное теоретическое исследование

Ab initio расчеты электронно-энергетической структуры и оптических свойств пироцирконатов лантана и неодима

А.А. Лаврентьев[1] ✉, Б.В. Габрельян[1], Ву Ван Туан[2], К.Ф. Калмыкова[1]

[1] Донской государственный технический университет, г. Ростов-на-Дону, Российская Федерация

[2] Институт вычислительной науки и искусственного интеллекта, Университет Ван Ланг, г. Хошимин, Вьетнам

✉ alavrentyev@donstu.ru

Аннотация

Введение. Соединения с лантаном и неодимом ($La_2Zr_2O_7$ и $Nd_2Zr_2O_7$) обладают низкой теплопроводностью, высокой диэлектрической проницаемостью и температурой плавления, стабильностью и устойчивостью к дефектам. Их можно применять для теплоизоляции металлических компонентов в турбинах и воздушных двигателях. Также указанные соединения широко исследуются с точки зрения развития материаловедения, в частности совершенствования лазерной техники и оптики. Однако физические свойства $La_2Zr_2O_7$ и $Nd_2Zr_2O_7$ недостаточно экспериментально изучены. Этот пробел призвано восполнить представленное исследование. Цель работы — модельные расчеты электронной структуры и оптических свойств $La_2Zr_2O_7$ и $Nd_2Zr_2O_7$.

Материалы и методы. На основе модельных расчетов в рамках теории функционала плотности исследована электронно-энергетическая структура пироцирконатов $La_2Zr_2O_7$ и $Nd_2Zr_2O_7$, содержащих Zr и имеющих кристаллическую структуру пирохлора. В расчетах использовались взятые из литературы параметры кристаллической решетки $La_2Zr_2O_7$. Из-за отсутствия экспериментальных данных параметры для $Nd_2Zr_2O_7$ рассчитывались через минимизацию сил, действующих на атомы соединения. Применяется комбинированный обменно-корреляционный потенциал, учитывающий сильные взаимодействия *d*- и *f*-электронов атомов La и Nd с поправкой в форме модифицированного метапотенциала Беке-Джонсона. Для расчетов использовался пакет программ *Wien2K*.

Результаты исследования. Получены плотности электронных состояний всех атомов исследованных соединений. Сравниваются рассчитанные плотности валентных электронных состояний соединений с экспериментальными рентгеновскими фотоэлектронными спектрами. При нулевой энергии рассчитаны значения оптических характеристик $La_2Zr_2O_7$ и $Nd_2Zr_2O_7$. Во-первых, это диэлектрическая проницаемость: для $La_2Zr_2O_7$ — 8,4334, для $Nd_2Zr_2O_7$ — 8,501. Во-вторых, преломление: для $La_2Zr_2O_7$ — 2,904, для $Nd_2Zr_2O_7$ — 2,916. В-третьих, отражение: для $La_2Zr_2O_7$ — 23,786 %, для $Nd_2Zr_2O_7$ — 23,935 %. Высокий оптический коэффициент поглощения ($>10^5$ см$^{-1}$) фиксируется в областях: от 5 до 14 эВ, от 14 до 28 эВ и от 28 до 40 эВ. Пиковые значения экстинкции приходятся на области от 5 до 13 эВ, от 14 до 28 эВ и от 28 до 40 эВ. Кристаллы $La_2Zr_2O_7$ и $Nd_2Zr_2O_7$ могут поглощать фотоны в широком диапазоне энергий (4–10 эВ).

Обсуждение и заключение. Исследование дополнило представления о свойствах $La_2Zr_2O_7$ и $Nd_2Zr_2O_7$ новыми экспериментальными данными. Рассчитаны плотности электронных состояний и оптические спектры соединений $La_2Zr_2O_7$ и $Nd_2Zr_2O_7$. Это позволило объяснить особенности экспериментальных рентгеновских фотоэлектронных спектров соединений. В приближении модифицированного потенциала Беке-Джонсона получены значения ширин запрещенных полос соединений, соответствующие экспериментальным. Исследование относится к фундаментальным и может открыть перспективы создания более эффективных, надежных и функциональных материалов, лазерных и оптических устройств.

Ключевые слова: электронная энергетическая структура, свойства группы пирохлоров, модифицированный метапотенциал Беке-Джонсона, оптические свойства $La_2Zr_2O_7$ и $Nd_2Zr_2O_7$

Благодарности. Авторы выражают благодарность рецензентам, чья критическая оценка представленных материалов и высказанные предложения по их совершенствованию способствовали значительному повышению качества статьи.

Для цитирования. Лаврентьев А.А., Габрельян Б.В., Туан Ву Ван, Калмыкова К.Ф. Ab initio расчеты электронно-энергетической структуры и оптических свойств пироцирконатов лантана и неодима. *Advanced Engineering Research (Rostov-on-Don).* 2025;25(2):129–141. https://doi.org/10.23947/2687-1653-2025-25-2-129-141

Introduction. Lanthanum and neodymium pyrozirconates — $La_2Zr_2O_7$ and $Nd_2Zr_2O_7$ — belong to the pyrochlores group. The general formula of these materials is $A_2B_2O_7$. *A* and *B* are metallic cations that can be trivalent (like La and Nd), tetravalent (like Zr), divalent, and pentavalent [1]. Pyrochlores have high dielectric constant. They exhibit unique magnetic [2], chemical, mechanical and electronic [3] properties. Due to this, they can be used as:

– ceramic coatings of thermal barriers, gas sensors, metal oxide transistors;

– solid electrolytes in fuel cells [4];

– immobilization carriers of actinides in nuclear waste;

– catalysts of oxidation reactions [5];

– elements of magnetic devices.

The research described in this paper was conducted taking into account the development of new technologies in the laser technology, optics and materials science [6]. The results of the work may open the way to the creation of more efficient, reliable and functional devices [7]. The studied oxides of complex chemical composition have significant stability, high melting point, high coefficient of thermal expansion [8], low thermal conductivity, excellent ionic conductivity, and resistance to defects [9]. From the practical perspective, it is important to use pyrochlores $Ln_2Zr_2O_7$ as coatings to provide thermal insulation of metal components from hot gases [10] in turbines of marine electric generators and in aircraft engines [11].

Numerous papers (e.g., [12]) investigated physical properties of pyrochlores, including mechanical and thermal ones. However, some of their properties are very difficult to evaluate and explain due to their strong dependence on the stoichiometry of the samples [10]. Calculations of the electron-energy structure of various pyrochlores were performed within the framework of the density functional theory (e.g., [13]). These calculations used exchange-correlation potentials obtained in the local density approximation, the generalized gradient approximation, and pseudopotentials.

In [13], the importance of the Hubbard correction in calculating the unoccupied *d*- and *f*-states of heavy atoms is noted [14]. Nevertheless, even taking into account the correction, the width of the forbidden band obtained in the calculations often turns out to be smaller than the experimentally observed one [15]. Additional corrections must be taken into account, and this is exactly what the authors of the presented work have done.

Thus, additional experimental and theoretical studies on the electron-energy structure and physical properties of pyrochlores are quite relevant and have practical significance.

Let us consider the crystal structure of pyrochlore $La_2Zr_2O_7$ (space group *Fd*-3*m*, Z = 8) with the general formula $Ln_2^{3+}Zr_2^{4+}O1_6O2$ (O1 and O2 are oxygen atoms located in different crystallographic positions). It can be described as a structure of defective fluorite, in which the cations form a face-centered cubic (*fcc*) lattice, and 1/8 of the oxygen atom positions are unoccupied to provide charge neutrality (Fig. 1).

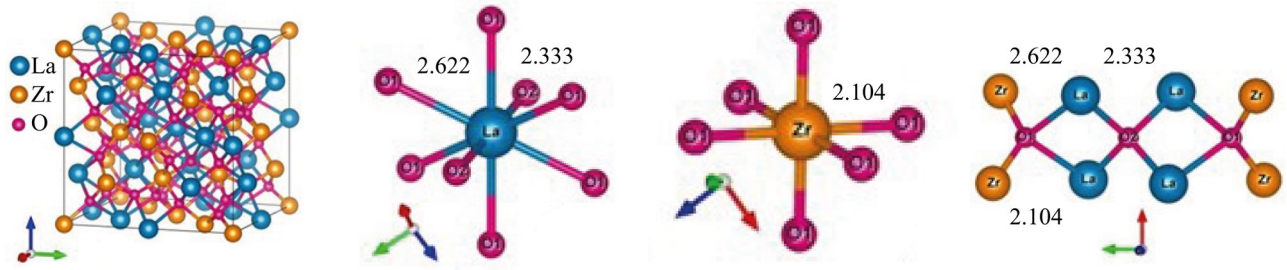

a) *b)* *c)* *d)*

Fig. 1. Crystal structure and immediate environment of atoms in pyrochlore $La_2Zr_2O_7$:
a — unit cell in compound $La_2Zr_2O_7$; *b* — immediate environment of La atom;
c — immediate environment of Zr atom; *d* — immediate environment of oxygen atoms O1 and O2.
Distances between atoms are given in Å

Atoms in the crystal structure of $La_2Zr_2O_7$ are distributed over four unique crystallographic positions:

– La cations are in Wyckoff positions 16*d*;

– Zr cations are in positions 16*c*;

– oxygen O1 is in position 48*f*;

– oxygen O2 is in position 8*b*.

The positions of 8*a* nodes (1/8, 1/8, 1/8) are not occupied at all. Oxygen ions O2 in 8*b* nodes (3/8, 3/8, 3/8) are stable and tetrahedrally coordinated by the rare earth element cations La.

Oxygen ions O1 in positions 48*f* (*x*, 1/8, 1/8) are shifted towards the neighboring empty nodes 8*a*, and they are surrounded by two La cations and two Zr cations (Fig. 1) [16]. The immediate environment of La cations consists of six oxygen atoms O1 (positions 48*f*) and two oxygen atoms O2 (positions 8*b*). La-O2 interatomic distance is shorter than La-O1 distance. Zr cations (Fig. 1) are surrounded by six O1 atoms (positions 48*f*), located at equivalent distances in trigonal antiprisms with 3*m* (D_{3d}) point symmetry.

The crystal structures of $Nd_2Zr_2O_7$ and $La_2Zr_2O_7$ compounds coincide. Table 1 shows the crystal lattice parameters of the studied pyrochlores $Ln_2Zr_2O_7$ (Ln = La, Nd) with the space group *Fd*-3*m*, for which $a = b = c$, $\alpha = \beta = \gamma = 90°$. For $La_2Zr_2O_7$, parameter *a* and the coordinates of oxygen O1 are taken from [15], and for $Nd_2Zr_2O_7$, they are calculated. The total energy of the crystal with different values of *a* was calculated, and the optimal value corresponding to the minimum of the total energy was determined. Then, the oxygen atoms were displaced within the unit cell and the position, for which the forces acting on the atoms became minimal, was determined.

Table 1

Crystal Structure Parameters of the Studied Compounds

Compound, lattice parameter	Wyckoff symbols	*x*/*a*	*y*/*b*	*z*/*c*
$La_2Zr_2O_7$ *a* = 10.793 Å [15]				
La	16*d*	0.50000	0.50000	0.50000
Zr	16*c*	0.00000	0.00000	0.00000
O1	48*f*	0.33002	0.12500	0.12500
O2	8*b*	0.37500	0.37500	0.37500
$Nd_2Zr_2O_7$ *a* = 10.6565 Å				
Nd	16*d*	0.50000	0.50000	0.50000
Zr	16*c*	0.00000	0.00000	0.00000
O1	48*f*	0.33520	0.12500	0.12500
O2	8*b*	0.37500	0.37500	0.37500

Thus, some physical properties of pyrochlores, as well as the structure of compounds $Nd_2Zr_2O_7$ and $La_2Zr_2O_7$, have been considered in scientific literature in sufficient detail. However, physical properties of $La_2Zr_2O_7$ and $Nd_2Zr_2O_7$ have not been sufficiently studied experimentally. The presented research is intended to fill this gap. The objective of the work is to perform model calculations of the electronic structure and optical properties of $La_2Zr_2O_7$ and $Nd_2Zr_2O_7$.

Materials and Methods. *Ab initio* calculations of the electron-energy structure (EES) of $La_2Zr_2O_7$ and $Nd_2Zr_2O_7$ were performed within the framework of the density functional theory. The method of augmented plane waves with the addition of local orbitals *APW+lo* was used. For the implementation, *WIEN*2*k* [17] software package was applied, which used a full potential that did not have a predetermined form, such as *muffin-tin* potential.

When constructing the attached plane wave, we used the expansion by *l* inside the atomic sphere up to $l_{max} = 10$. The following radii of the atomic spheres were used in the present calculations: $R_{(La)} = 2.24$ *a.u.*, $R_{(Nd)} = 2.26$ *a.u.*, $R_{(Zr)} = 1.96$ *a.u.*, $R_{(O)} = 1.78$ *a.u.* (1 *a.u.* = 0.529117 *Å*). The series of the expansion in plane waves was interrupted at the values of the wave vector determined by the relation $R_{min}^{MT} k_{max} = 7$, where R_{min} — radius of the minimal atomic sphere. The charge density decomposed into a Fourier series up to value $G_{max} = 12$ $(a.u)^{-1}$. The densities of electron states were obtained through integrating over 1,000 $\vec{k}$ points in the irreducible Brillouin zone (BZ) using the tetrahedron method [18]. The self-consistency procedure was carried out until the change in the integral charge $q = \int|\rho_n - \rho_{n-1}|dr$ became less than $q \leq 0.0001$. Here, $\rho_{n-1}(r)$ and $\rho_n(r)$ are the electron densities obtained at iterations n–1 and n, respectively.

To calculate the exchange-correlation potential, the following were used:

– generalized gradient approximation (GGA) in the parameterization proposed in [19];

– modified Becke-Johnson potential, *mBJ* [20].

In addition to the above exchange-correlation potentials, the EES calculations took into account the strong Coulomb interaction of *f*- electrons at one node Nd [21] in *PBE+U* approximation [22] with $U = 5eV$. Thus, in the final version, the exchange-correlation potential models were used *PBE+U* and *mBJ+U* [23].

$Nd_2Zr_2O_7$ has an incomplete 4*f*-shell with four *f*-electrons, therefore, a spin-polarized EES calculation was performed. For La, Nd and Zr atoms, spin-orbit coupling (SOC) was taken into account. It resulted in splitting:

– 5*p*-states of La and Nd into $5p_{1/2}$ and $5p_{3/2}$ states;

– $4p^6$-states of Zr into $4p_{1/2}$ and $4p_{3/2}$ states.

Research Results. The paper calculates the total and partial densities of electron states (DOS). Atom La has no *f*-electrons, while atom *Nd* has four *f*-electrons. Despite this difference, in the first approximation, the calculated total densities of electron states and the experimental X-ray photoelectron spectra of the valence bands of the studied compounds demonstrate a similar structure — four regions reflecting the contributions of *s*-, *p*-, *d*- and *f*-electrons of different elements [23].

Figure 2 provides comparing the experimental X-ray photoelectron spectrum (XPS) to the calculated total and partial densities DOS for compound $La_2Zr_2O_7$, and Figures 3–5 — for $Nd_2Zr_2O_7$. Zero of the energy scale corresponds to the top of the valence band E_V. The spectra were obtained at the Frantsevich Institute for Problems of Materials Science, National Academy of Sciences of Ukraine (Kyiv). The experimental features and equipment are described in [24].

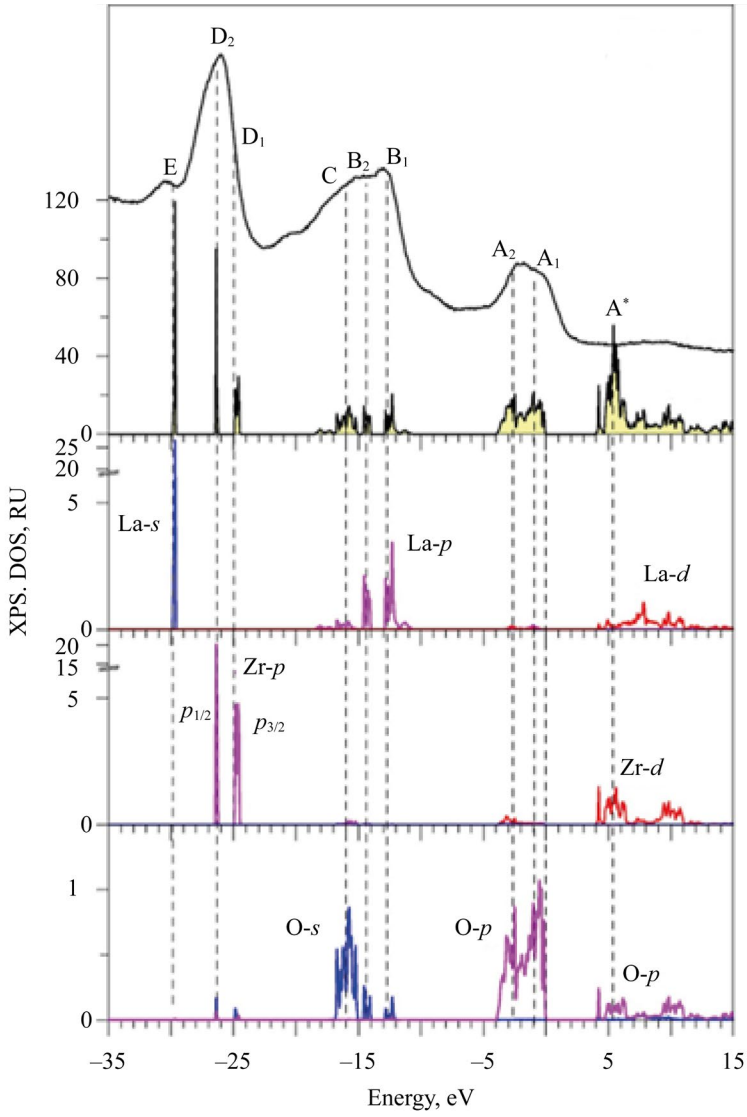

Fig. 2. Total and partial densities of states (DOS) calculated in *GGA–PBE–SOC* approximation in comparison with experimental X-ray photoelectron spectrum (XPS) of valence band of compound $La_2Zr_2O_7$

In Figure 2, in compound $La_2Zr_2O_7$, region 1 is shown— the upper part of the valence band from 0 to 4 eV. This region is formed mainly by 2*p*-states of oxygen with a small admixture of 4*d*-states of Zr, 5*s*-states of *Zr*, and 6*s*- and 5*d*-states of La.

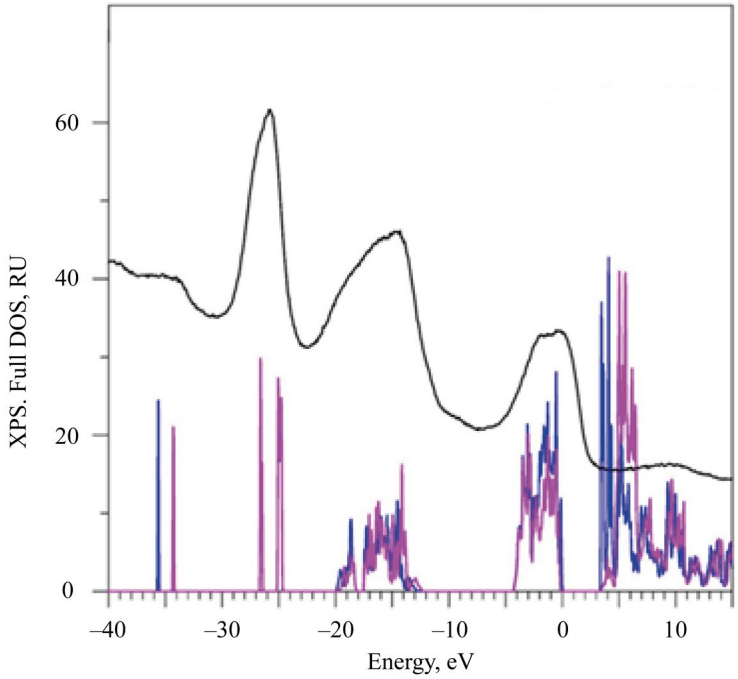

Fig. 3. Total densities of states (DOS) calculated in *GGA–PBE+U+SOC* approximation with spin up and spin down in comparison with the experimental X-ray photoelectron spectrum (XPS)

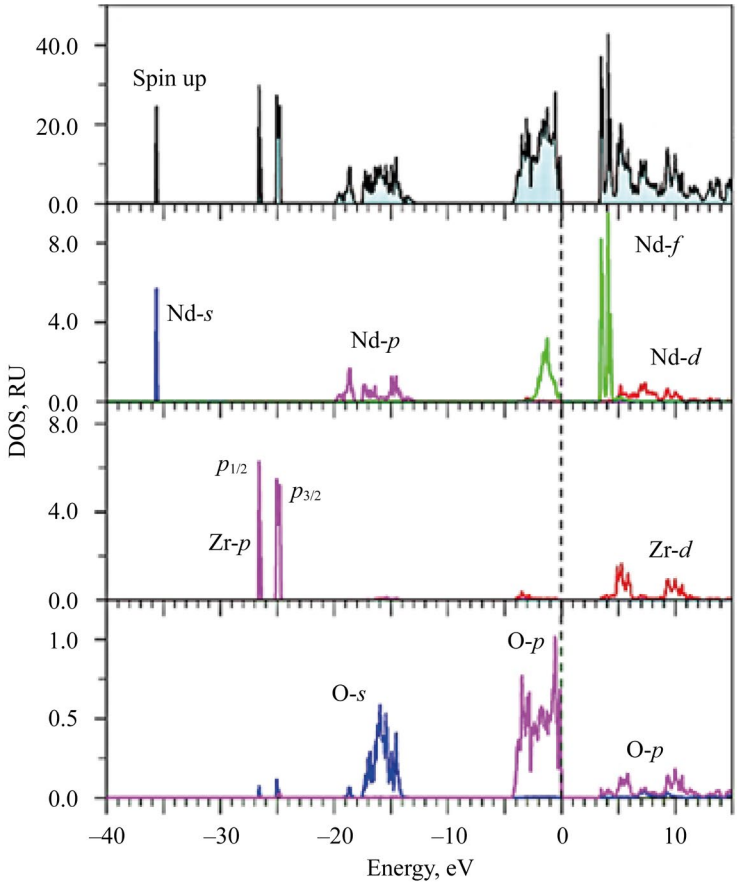

Fig. 4. Total and partial densities of states (DOS) of electrons for spin up in $Nd_2Zr_2O_7$ calculated in *GGA–PBE+U+SOC* approximation

Here, in $Nd_2Zr_2O_7$, at the top of the valence band, *f*-states of *Nd* with spin up are located. X-ray photoelectron spectrum (XPS) confirms the calculation. It is seen that the broad peak closest to the top of the valence band with elements A_1 and A_2 in $La_2Zr_2O_7$ and A in $Nd_2Zr_2O_7$ corresponds to 2*p*-states of oxygen atoms O1 and O2.

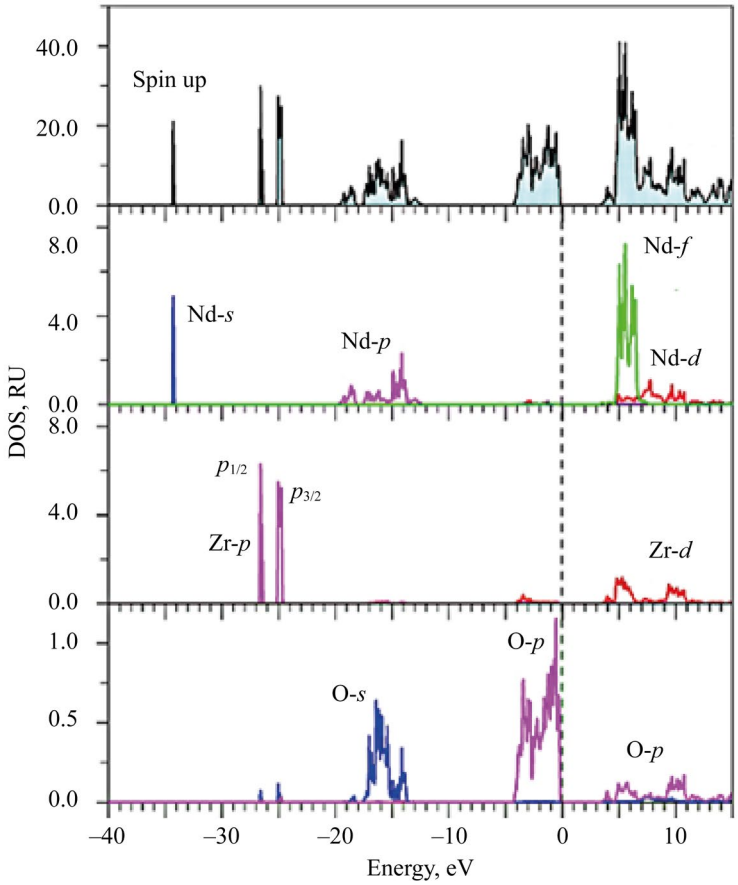

Fig. 5. Total and partial densities of states (DOS) of electrons for spin down in $Nd_2Zr_2O_7$ calculated in *GGA–PBE+U+SOC* approximation

In regions 2, 12–18 eV from E_v in XPS, there is also a broad peak with features B_1, B_2 and C for $La_2Zr_2O_7$ and B for $Nd_2Zr_2O_7$. The theoretical calculation shows the entire fine structure that forms the peak in XPS. $5p^6$-states of La and Nd are split into $5p_{1/2}$- and $5p_{3/2}$-states. This splitting is already evident in free atoms La and Nd [25].

The spin-orbit splitting in a free atom is also present in a solid (Fig. 2) in the third panel from the bottom for the partial states of La. It is the spin-orbit splitting of the 5*p*-states of La that leads to the splitting of the 2*s*-states of oxygen. This is clearly seen in the very bottom panel of Figure 2, where the partial states of oxygen are shown. As Figure 2 shows, in the energy region ~12–18 eV, the deep-lying 5*p*-states of La interact with the 2*s*-states of oxygen. This interaction of deep-lying states in a solid is unusual and is related primarily to:

– spin-orbit splitting of the 5*p*-states of La;

– the fact that the 2*s*-wave function of oxygen is spatially and energetically strongly stretched.

The presence of structural elements B_1, B_2 and C in the X-ray photoelectron spectrum coincides well with the calculations of the peak in the partial densities of the electron states of La and O.

The third energy region (from 24 to 27 eV) from E_v — peaks D_1 and D_2 in the X-ray photoelectron spectrum of $La_2Zr_2O_7$, C — in the spectrum of $Nd_2Zr_2O_7$. This region corresponds to the 4*p*-states of Zr, which are split in the atom into:

– $4p_{1/2}$-state with energy 35 eV (N_2);

– $4p_{3/2}$-states with energy 33 eV (N_3).

In the XPS curve of $La_2Zr_2O_7$, the splitting of the 4*p*-states of Zr is manifested as an asymmetry of the lines with elements D_1 and D_2.

The deepest states of the valence bands of $La_2Zr_2O_7$ and $Nd_2Zr_2O_7$ are already semi-core states. The fourth energy region in the XPS spectrum (small peak E in Fig. 2, 3) is the 5*s*-states of La and Nd. Note that La 5*s*-state in $La_2Zr_2O_7$ is not split compared to the 5s-states of Nd with different spin directions (Fig. 3). The splitting of the 5*s*-states of *Nd* for spin up and spin down occurs under the action of the internal magnetic field. It is created by four 4*f*-electrons, which are aligned identically with spin up according to Hund's rule [26]. The broad influx of D in the XPS spectrum (Fig. 3) corresponds to the 5*s*-states of Nd.

The energy distribution of the electron states in the valence band $La_2Zr_2O_7$ correlates well with the electronegativity (EN) values of the elements [27] included in this compound (Table 2).

Table 2

Electronegativity of Elements Included in the Compounds under Study [27]

Element	O	Zr	La	Nd	Sm	Eu	Gd
EN	3.44	1.33	1.10	1.14	1.17	1.20	1.20

Thus, oxygen has the highest EN (3.44), therefore, it is quite natural that the upper part of the valence band is formed by the 2*p*-state of O. The admixture of the 4*d*- and 5*s*-states of Zr to the 2*p*-states of oxygen is insignificant, since the Zr-O1 bond is predominantly ionic in nature. The electronegativity of oxygen (EN = 3.44) is significantly higher than that of Zr (EN = 1.33). Due to this, the 4*d*- and 5*s*-electron densities of Zr are apparently attracted to the oxygen atom (O1), which is typical for the octahedral environment of the Zr atom by O1 atoms. There are also six O1 atoms in the environment of the La atom. The electronegativity of La (EN = 1.1) is significantly less than $EN^S = 3.44$. Admixture of 5*d*- and 6*s*-states of La is almost not observed. The bond between La and O1 atoms is predominantly ionic in nature, the share of covalence in this bond is very small.

The bottom of the conduction band in both compounds is formed mainly by unoccupied *f*- and *d*-states of La/Nd, as well as *d*-states of Zr (Fig. 2, 4, 5).

A well-known problem of calculations using the exchange-correlation potential in the *GGA*-approximation is the underestimation of the obtained value of the band gap. For some non-conducting compounds, the calculations even give a conducting state or, as in the case of $Nd_2Zr_2O_7$ in this calculation, a zero value of the band gap. Taking into account the strong interaction of *f*- electrons in *Nd* atom, e.g., within the framework of the *LDA+U* (or *GGA+U*) approximation in the EES calculations of $Nd_2Zr_2O_7$, leads to the appearance of a small forbidden band, but the value close to the experimental one can be obtained either in calculation schemes that consider multi-electron phenomena, or by using hybrid or metapotentials, such as the modified Becke-Johnson potential (*mBJ*) [28].

Table 3 gives the values of the widths of the forbidden bands E_g. They were calculated taking into account the spin-orbit splitting (SOC) of the electron states in the *La* and *Nd* atoms in the *GGA–PBE* approximations for $La_2Zr_2O_7$ (*GGA–PBE+SOC*) and *GGA+PBE+U+SOC* (with $U = 5eV$ for 4*f*-states of *Nd*) for $Nd_2Zr_2O_7$.

Table 3

Calculated Values of the Widths of Prohibited Bands E_g

Compound	Exchange-correlation potential	E_g, eV
$La_2Zr_2O_7$	*GGA–PBE+SOC*	3.928
$Nd_2Zr_2O_7$	*GGA–PBE+U+SOC*	3.393

The complex dielectric function $\varepsilon(\omega) = \varepsilon_1(\omega) + i\varepsilon_2(\omega)$ — the most important characteristic for calculating the optical response of materials to electromagnetic impact. The dielectric function, in principle, should include both transitions between bands and transitions within a band. Interband transitions are divided into direct and indirect. In these calculations, two factors are ignored. The first is intraband transitions, since they are important for metals, and the compounds under study are semiconductors. The second is the contribution of phonons and other quasiparticles included in indirect interband transitions. Only direct transitions between occupied and unoccupied states are considered. The cubic symmetry of the pyrochlore crystal structure determines only three non-zero (diagonal) elements of the dielectric tensor, and the values of all three of these elements are the same.

The calculated curves of the actual $\varepsilon_1(\omega)$ and imaginary $\varepsilon_2(\omega)$ parts of the permittivity for $La_2Zr_2O_7$ and $Nd_2Zr_2O_7$ are shown in Figure 6.

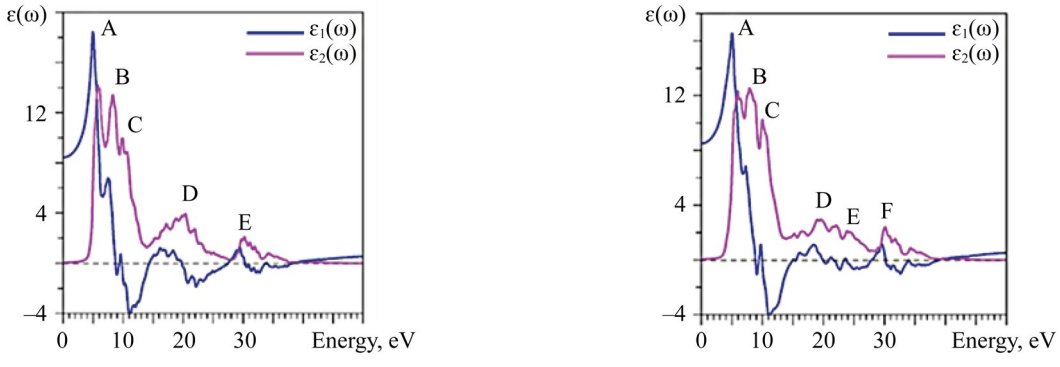

a) *b)*

Fig. 6. Calculated actual (ε_1) and imaginary parts of permittivity: *a* — $La_2Zr_2O_7$; *b* — $Nd_2Zr_2O_7$

The spectral peaks of the absorbing part of the dielectric function correspond to the allowed dipole transitions between the valence band and the conduction band. To identify the fine structure elements, it is required to compare the values of the optical matrix elements. The observed structures correspond to those transitions that have large values of the optical matrix dipole transition elements. When calculating $\varepsilon_2(\omega)$, only dipole transitions within the atom, i.e., without crossover transitions, were taken into account. The interpretation of peaks *A*, *B*, *C*, *D*, *E*, *F* in Figure 6 for $\varepsilon_2(\omega)$ is given in Table 4.

Table 4

Interpretation of Major Peaks $\varepsilon_2(\omega)$

Compound	Peak	Energy, eV	Atom	Transition
$La_2Zr_2O_7$	*A*	≈ 5	O	$p \rightarrow s(d)$
	B	≈ 8	O	$p \rightarrow s$
	C	≈ 10	O	$p \rightarrow s$
	D	≈ 20	O La	$p \rightarrow s$ $5p \rightarrow d$
	E	≈ 30	Zr	$4p \rightarrow d$
$Nd_2Zr_2O_7$	*A*	5.07	O	$p \rightarrow s$
	B	7.8	O	$p \rightarrow s$
	C	10.2	O	$p \rightarrow s$
	D *E*	19.09 24.02	O Nd	$p \rightarrow s$ $5p \rightarrow d$
	F	30.11	Zr	$4p \rightarrow d$

Figure 6 shows the process when electrons of *p*-symmetry in the upper part of the valence band (peak *A* in XPS) pass to states of *s*- and *d*-symmetry in the conduction band of the oxygen atom. This is how the highest peak of the curve of the imaginary part of the dielectric function $\varepsilon_2(\omega)$ is formed, covering the range 5–8 eV.

The second and third highest peaks of the curve $\varepsilon_2(\omega)$ — *B* and *C* with energies 8.28 and 9.86 eV, respectively. They are caused by transitions of oxygen valence *p*- electrons to free states of oxygen *s*-symmetry. Let us consider the wide maximum *D* on the curve $\varepsilon_2(\omega)$. The "picket-fence" of small additional peaks appeared due to transitions of oxygen *s*-symmetry electrons to free states of oxygen *p*-symmetry. In addition, in peak *D* (energy~20 eVB), there is a contribution from the transitions of the valence 5*p*-electrons of *La* to the vacant *d*-states of La in the conduction band. Finally, small peak *E* (energy~30 eV) corresponds to the transition of the valence 4*p*-electrons of Zr to the unoccupied *d*-states of Zr. At zero energy, the calculated value $\varepsilon_2(0)$ for $La_2Zr_2O_7$ is 8.4334, and for $Nd_2Zr_2O_7$ — 8.501.

All other optical properties can be derived from $\varepsilon_1(\omega)$ and $\varepsilon_2(\omega)$. These include, for example: absorption coefficient $\alpha(\omega)$, refractive index $n(\omega)$, extinction coefficient $k(\omega)$, optical reflectivity $R(\omega)$, and energy loss spectrum $L(\omega)$ [28].

The high optical absorption coefficient $\alpha(\omega) > 10^5$ cm^{-1} [29] is recorded in three clearly defined regions: from 5 to 14 eV, from 14 to 28 eV and from 28 to 40 eV (Fig. 7). Apparently, such absorption may indicate the potential of using thin-film elements from $La_2Zr_2O_7$ and $Nd_2Zr_2O_7$.

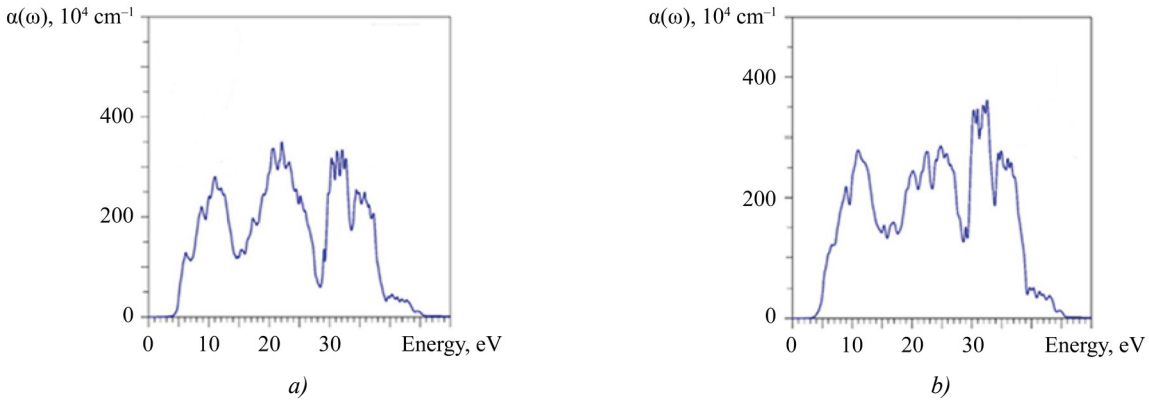

Fig. 7. Calculated absorption coefficient $\alpha(\omega)$: *a* — $La_2Zr_2O_7$; *b* — $Nd_2Zr_2O_7$

In addition, the optical absorption spectrum is characterized by a large number of peaks. They are formed due to transitions between occupied levels of the valence band and free levels of the conduction band, allowed by the selection rules ($\Delta l \neq 0$) and related to one atom (cross-transitions between neighboring atoms are unlikely). Such a picket-fence of small peaks on the curve $a(\omega)$ is undoubtedly related to the features of the above-described electron-energy structure of $La_2Zr_2O_7$ and $Nd_2Zr_2O_7$. Probably, it should be taken into account when using these compounds in optoelectronics.

The complex refractive index $N(\omega) = n(\omega) + ik(\omega)$ can be obtained from the complex dielectric function $\varepsilon(\omega)$, where the refractive index $n(\omega)$ depends mainly on the actual part $\varepsilon_1(\omega)$, and the extinction coefficient $k(\omega)$ depends on the imaginary part of the dielectric function $\varepsilon_2(\omega)$ [30].

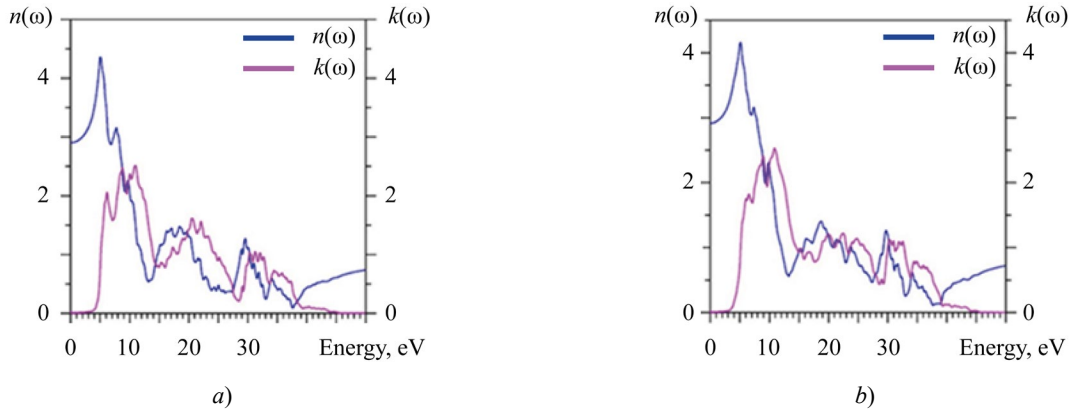

Fig. 8. Calculated refractive index $n(\omega)$ and extinction coefficient $k(\omega)$: *a* — $La_2Zr_2O_7$; *b* — $Nd_2Zr_2O_7$

At zero energy, the calculated value $n(0)$ (static refractive index) for $La_2Zr_2O_7$ is 2.904, and for $Nd_2Zr_2O_7$ — 2.916.

The extinction coefficient $k(\omega)$, responsible for the absorption of the electromagnetic wave incident on the crystal, is obtained from the imaginary part of the dielectric function $\varepsilon_2(\omega)$ (Fig. 6). Therefore, there are also three regions where value $k(\omega)$ increases from 5 to 13 eV, from 14 to 28 eV and from 28 to 40 eV. The attenuation of the intensity, represented by the extinction coefficient $k(\omega)$, starts with a decrease in the function $n(\omega)$ (Figc. 8). $La_2Zr_2O_7$ and $Nd_2Zr_2O_7$ crystals can absorb photons in a wide energy range (4–10 eV).

In general, the extinction coefficient of $La_2Zr_2O_7$ and $Nd_2Zr_2O_7$ is not isotropic and has three well-defined regions (energies are given above) where isotropic behavior of $k(\omega)$ is not observed. In these regions, the difference in $k(\omega)$ values is 25–50%.

The reflection coefficient $R(\omega)$ is shown in Figure 9. The spectrum $R(\omega)$ consists of three clearly defined energy regions. The same feature was noted for other optical characteristics. At zero energy, the calculated value $R(0)$ for $La_2Zr_2O_7$ is 23.786%, and for $Nd_2Zr_2O_7$ — 23.935%.

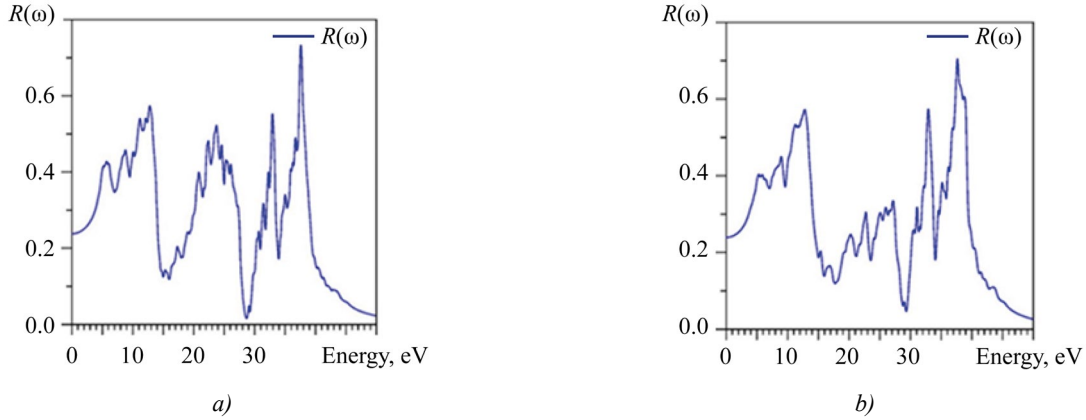

Fig. 9. Calculated reflection coefficient $R(\omega)$: *a* — $La_2Zr_2O_7$; *b* — $Nd_2Zr_2O_7$

It is evident from Figure 8 that incident photons with energy lower than the energy of the forbidden gap (~4 eV) are not absorbed. Photons with energy from 4 eV to~40 eV are absorbed by $La_2Zr_2O_7$, $Nd_2Zr_2O_7$ crystals and excite electrons in the conduction band, while positively charged holes are formed in the valence band. However, part of the photon energy will be lost during thermalization, and it is reflected in the electron energy loss spectrum $L(\omega)$ shown in Figure 10.

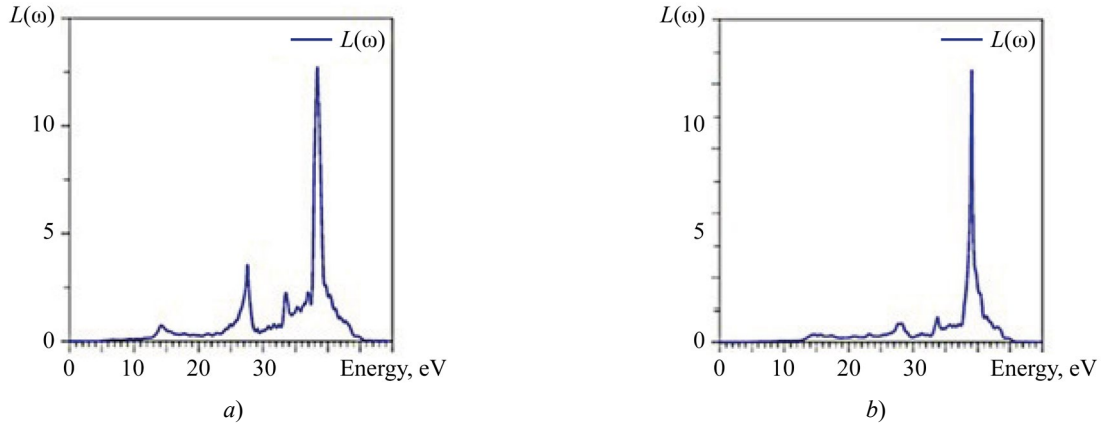

Fig. 10. Calculated spectrum of electron energy losses: *a* — $La_2Zr_2O_7$; *b* — $Nd_2Zr_2O_7$

The energy loss of the electron becomes significant at 14 eV (small peak),~27 eV,~33.5 eV. The largest value $L(\omega)$ is reached at 39 eV, which corresponds to a sharply decreasing edge of the absorption coefficient $a(\omega)$ (Fig. 7).

Discussion and Conclusion. The calculation of the electron density states of the valence bands of $La_2Zr_2O_7$, $Nd_2Zr_2O_7$ gave two results:

– allowed us to explain all the main features of the experimental X-ray photoelectron spectra of these compounds in the energy range of ~35 eV from the top of the valence band;

– showed which electron symmetry determined the main features of the experimental spectra.

Together with the obtained densities of unoccupied states, the calculated densities of occupied states allowed us to define the optical coefficients of the compounds studied. It is extremely important to take into account the corrections in the exchange-correlation part of the potential (*GGA+U*, *mBJ*). Only with them it is possible to obtain the values of the widths of the forbidden bands that correspond to the experimental data. For $Nd_2Zr_2O_7$, calculations without corrections generally show a non-zero density of states at the Fermi level.

References

1. Chartier A, Meis C, Crocombette J, Corrales LR, Weber WJ. Atomistic Modeling of Displacement Cascades in $La_2Zr_2O_7$ Pyrochlore. *Physical Review B*. 2003;67:174102. https://doi.org/10.1103/PhysRevB.67.174102

2. Stanek CR, Minervini L, Grimes RW. Nonstoichiometry in $A_2B_2O_7$ Pyrochlores. *Journal of the American Ceramic Society*. 2002;85(11):2792–2798. https://doi.org/10.1111/j.1151-2916.2002.tb00530.x

3. Pirzada M, Grimes RW, Minervini L, Maguire JF, Sickafus KE. Oxygen Migration in $A_2B_2O_7$ Pyrochlores. *Solid State Ionics*. 2001;140:201–208. https://doi.org/10.1016/S0167-2738(00)00836-5

4. Tabira Y, Withers RL, Minervini L, Grimes RW. Systematic Structural Change in Selected Rare Earth Oxide Pyrochlores as Determined by Wide-Angle CBED and a Comparison with the Results of Atomistic Computer Simulation. *Journal of Solid State Chemistry*. 2000;153(1):16–25. https://doi.org/10.1006/jssc.2000.8712

5. Helean KB, Ushakov SV, Brown CE, Navrotsky A, Lian J, Ewing RC, et al. Formation Enthalpies of Rare Earth Titanate Pyrochlores. *Journal of Solid State Chemistry*. 2004;177(6):1852–1866. https://doi.org/10.1016/j.jssc.2004.01.009

6. Lian J, Zu XT, Kutty KVG, Chen J, Wang LM, Ewing RC. Ion-Irradiation-Induced Amorphization of $La_2Zr_2O_7$ Pyrochlore. *Physical Review B*. 2002;66:054108. https://doi.org/10.1103/PhysRevB.66.054108

7. Chen J, Lian J, Wang LM, Ewing RC, Wang RG, Pan W. X-ray Photoelectron Spectroscopy Study of Disordering in $Gd_2(Ti_{1-x}Zr_x)_2O_7$ Pyrochlores. *Physical Review Letters*. 2002;88:105901. https://doi.org/10.1103/PhysRevLett.88.105901

8. Yong Jiang, Smith JR, Odette GR. Prediction of Structural, Electronic and Elastic Properties of $Y_2Ti_2O_7$ and Y_2TiO_5. *Acta Materialia*. 2010;58(5):1536–1543. https://doi.org/10.1016/j.actamat.2009.10.061

9. Winter MR, Clarke DR. Thermal Conductivity of Yttria-Stabilized Zirconia-Hafnia Solid Solutions. *Acta Materialia*. 2006;54(19):5051–5059. https://doi.org/10.1016/j.actamat.2006.06.038

10. Matteucci F, Cruciani G, Dondi M, Baldi G, Barzanti A. Crystal Structural and Optical Properties of Cr-Doped $Y_2Ti_2O_7$ and $Y_2Sn_2O_7$ Pyrochlores. *Acta Materialia*. 2007;55(7):2229–2238. https://doi.org/10.1016/j.actamat.2006.11.008

11. Uno M, Kosuga A, Okui M, Horisaka K, Muta H, Kurosaki K, et al. Photoelectrochemical Study of Lanthanide Zirconium Oxides, $Ln_2Zr_2O_7$ (Ln = La, Ce, Nd and Sm). *Journal of Alloys and Compounds*. 2006;420:291–297. https://doi.org/10.1016/j.jallcom.2005.10.072

12. Ciomaga Hatnean M, Lees MR, Balakrishnan G. Growth of Single-Crystals of Rare-Earth Zirconate Pyrochlores, $Ln_2Zr_2O_7$ (with Ln = La, Nd, Sm, and Gd) by the Floating Zone Technique. *Journal of Crystal Growth*. 2015;418:1–6. https://doi.org/10.1016/j.jcrysgro.2015.01.037

13. Feng J, Xiao B, Wan CL, Qu ZX, Huang ZC, Chen JC, et al. Electronic Structure, Mechanical Properties and Thermal Conductivity of $Ln_2Zr_2O_7$ (Ln = La, Pr, Nd, Sm, Eu and Gd) Pyrochlore. *Acta Materialia*. 2011;59(4):1742–1760. https://doi.org/10.1016/j.actamat.2010.11.041

14. Zheng Li, Wei Pan. Electronic Structure and Transport Properties of $La_2Zr_2O_7$ Pyrochlore from First Principles. *Solid State Phenomena*. 2018;281:767–773. https://doi.org/10.4028/www.scientific.net/SSP.281.767

15. Liu B, Wang JY, Zhou YC, Liao T, Li FZ. Theoretical Elastic Stiffness, Structure Stability and Thermal Conductivity of $La_2Zr_2O_7$ Pyrochlore. *Acta Materialia*. 2007;55(9):2949–2957. https://doi.org/10.1016/j.actamat.2006.12.035

16. Subramanian MA, Aravamudan G, Subba Rao GV. Oxide Pyrochlores — A Review. *Progress in Solid State Chemistry*. 1983;15(2):55–143. https://doi.org/10.1016/0079-6786(83)90001-8

17. Blaha P, Schwarz K, Tran F, Laskowski R, Madsen GKH, Marks LD. WIEN2k: an APW+lo Program for Calculating the Properties of Solids. *Journal of Chemical Physics*. 2020;152(7):074101. https://doi.org/10.1063/1.5143061

18. Blöchl PE, Jepsen O, Andersen OK. Improved Tetrahedron Method for Brillouin-Zone Integrations. *Physical Review B*. 1994;49(23):16223–16233. https://doi.org/10.1103/PhysRevB.49.16223

19. Perdew JP, Burke K, Ernzerhof M. Generalized Gradient Approximation Made Simple. *Physical Review Letters*. 1996;77(18):3865–3868. https://doi.org/10.1103/PhysRevLett.77.3865

20. Tran F, Blaha P. Accurate Band Gaps of Semiconductors and Insulators with a Semilocal Exchange-Correlation Potential. *Physical Review Letters*. 2009;102(22):226401. https://doi.org/10.1103/PhysRevLett.102.226401

21. Anisimov VI, Solovyev IV, Korotin MA, Czyżyk MT, Sawatzky GA. Density-Functional Theory and NiO Photoemission Spectra. *Physical Review B*. 1993;48(23):16929–16934. https://doi.org/10.1103/PhysRevB.48.16929

22. Novák P, Boucher F, Gressier P, Blaha P, Schwarz K. Electronic Structure of the Mixed Valence System $(YM)_2BaNiO_5$ (M = Ca, Sr). *Physical Review B*. 2001;63(23):235114. https://doi.org/10.1103/PhysRevB.63.235114

23. Hong Jiang. Band Gaps from the Tran-Blaha Modified Becke-Johnson Approach: A Systematic Investigation. *The Journal of Chemical Physics*. 2013;138(13):134115. https://doi.org/10.1063/1.4798706

24. Tuan V Vu, Khyzhun OY, Lavrentyev AA, Gabrelian BV, Kalmykova KF, Isaenko LI, et al. Electronic Band Structure and Optical Properties of $Li_2In_2GeSe_6$ Crystal. *Materials Today Communications*. 2023;35:105798. https://doi.org/10.1016/j.mtcomm.2023.105798

25. Lotz W. Electron Binding Energies in Free Atoms. *The Journal of the Optical Society of America*. 1970:60(2):206–210.

26. Lide DR (ed). *CRS Handbook of Chemistry and Physics*. 87th ed. Boca Raton; London; New York: CRC Press; Taylor & Francis; 2007. 2608 p.

27. Ambrosch-Draxl C, Sofo JO. Linear Optical Properties of Solids within the Full-Potential Linearized Augmented Planewave Method. *Computer Physics Communications*. 2006;175(1):1–14. https://doi.org/10.1016/j.cpc.2006.03.005

28. Khan SA, Reshak AH. Optoelectronic and Transport Properties of Zintl Phase $KBa_2Cd_2Sb_3$ Compound. *Computational Materials Science*. 2014;95:328–336. https://doi.org/10.1016/j.commatsci.2014.07.031

29. Boujnah M, Dakir O, Zaari H, Benyoussef A, Kenz AE. Optoelectronic Response of Spinels CdX2O4 with X = (Al, Ga, In) through the Modified Becke-Johnson Functional. *Journal of Applied Physics*. 2014;116(12):123703. https://doi.org/10.1063/1.4896110

30. Tuan V Vu, Lavrentyev AA, Doan V Thuan, Chuong V Nguyen, Khyzhun OY, Gabrelian BV, et al. Electronic Properties and Optical Behaviors of Bulk and Monolayer ZrS_2: A Theoretical Investigation. *Superlattices and Microstructures*. 2019;125:205–213. https://doi.org/10.1016/j.spmi.2018.11.008

About the Authors:

Anatoliy A. Lavrentyev, Dr.Sci. (Phys.-Math.), Professor, Head of the Electrical Engineering and Electronics Department, Don State Technical University (1, Gagarin Sq., Rostov-on-Don, 344003, Russian Federation), SPIN-code, ORCID, ScopusID, ResearchGate, alavrentyev@donstu.ru

Boris V. Gabrelian, Cand.Sci. (Phys.-Math.), Associate Professor of the Computer and Automated Systems Software Department, Don State Technical University (1, Gagarin Sq., Rostov-on-Don, 344003, Russian Federation), SPIN-code, ORCID, ScopusID, ResearcherID, boris.gabrelian@gmail.com

Vu Van Tuan, Cand.Sci. (Phys.-Math.), Leading Researcher, Laboratory of Computational Physics, Institute of Computational Science and Artificial Intelligence, Van Lang University (69/68, Dang Thuy Tram Str. Ward 13, Binh Thanh District, Ho Chi Minh City, 70000, Vietnam), ORCID, ScopusID, vuvan.tuan@mail.ru

Ksenia F. Kalmykova, Teaching Assistant of the Electrical Engineering and Electronics Department, Don State Technical University (1, Gagarin Sq., Rostov-on-Don, 344003, Russian Federation), SPIN-code, ORCID, ScopusID, ResearchGate, 16ksy16@mail.ru

Claimed contributorship:
AA Lavrentyev: conceptualization, supervision, project administration.
BV Gabrelian: methodology, formal analysis, data curation, validation.
Vu Van Tuan: resources, validation, writing – original draft preparation.
KF Kalmykova: formal analysis, writing – review and editing.

Conflict of Interest Statement: **the authors declare no conflict of interest.**

All authors have read and approved the final version of manuscript.

Об авторах:
Анатолий Александрович Лаврентьев, доктор физико-математических наук, профессор, заведующий, кафедра «Электротехника и электроника» Донского государственного технического университета (344003, Российская Федерация, г. Ростов-на-Дону, пл. Гагарина, 1), SPIN-код, ORCID, ScopusID, ResearchGate, alavrentyev@donstu.ru

Борис Витальевич Габрельян, кандидат физико-математических наук, доцент, кафедра «Программное обеспечение вычислительной техники и автоматизированных систем» Донского государственного технического университета (344003, Российская Федерация, г. Ростов-на-Дону, пл. Гагарина, 1), SPIN-код, ORCID, ScopusID, ResearcherID, boris.gabrelian@gmail.com

Ву Ван Туан, кандидат физико-математических наук, ведущий научный сотрудник, «Лаборатория вычислительной физики» института вычислительной науки и искусственного интеллекта, Университет Ван Ланг, Хошимин, Вьетнам, ORCID, ScopusID, vuvan.tuan@mail.ru

Ксения Федоровна Калмыкова, ассистент, кафедра «Электротехника и электроника» Донского государственного технического университета (344003, Российская Федерация, г. Ростов-на-Дону, пл. Гагарина, 1), SPIN-код, ORCID, ScopusID, ResearchGate, 16ksy16@mail.ru

Заявленный вклад авторов:
А.А. Лаврентьев: разработка концепции, научное руководство, административное руководство исследовательским проектом.
Б.В. Габрельян: разработка методологии, формальный анализ, курирование данных, валидация результатов.
Ву Ван Туан: предоставление ресурсов, валидация результатов, написание черновика рукописи.
К.Ф. Калмыкова: формальный анализ, написание рукописи – рецензирование и редактирование.

Конфликт интересов: **авторы заявляют об отсутствии конфликта интересов.**

Все авторы прочитали и одобрили окончательный вариант рукописи.

Received / **Поступила в редакцию** 10.03.2025
Reviewed / Поступила после рецензирования 03.04.2025
Accepted / **Принята к публикации** 14.04.2025